

ImmunoHorizons CALL FOR IMMUNOLOGY EDUCATION PAPERS!

Visit ImmunoHorizons.org for more information!



RESEARCH ARTICLE | FEBRUARY 14 2024

TCDD and CH223191 Alter T Cell Balance but Fail to Induce Anti-Inflammatory Response in Adult Lupus Mice

Fernando Gutierrez; ... et. al

Immunohorizons (2024) 8 (2): 172-181.

https://doi.org/10.4049/immunohorizons.2300023

Related Content

AhR Activation Leads to Massive Mobilization of Myeloid-Derived Suppressor Cells with Immunosuppressive Activity through Regulation of CXCR2 and MicroRNA miR-150-5p and miR-543-3p That Target Anti-Inflammatory Genes

J Immunol (October,2019)

2,3,7,8-tetrachlorodibenzo-p-dioxin (TCDD) induces tolerance by altering the gut microbiome

J Immunol (May,2017)

Effect of AhR activation by TCDD on the immunosuppressive CTLA-4 - IFNγ - IDO pathway (176.5)

J Immunol (May,2012)



TCDD and CH223191 Alter T Cell Balance but Fail to Induce Anti-Inflammatory Response in Adult Lupus Mice

Fernando Gutierrez,*^{1,2} Quiyana M. Murphy,^{†,2} Brianna K. Swartwout,^{‡,2} Kaitlin A. Read,* Michael R. Edwards,* Leila Abdelhamid,* Xavier Cabana-Puig,* James C. Testerman,* Tian Xu,* Ran Lu,* Pavly Amin,* Thomas E. Cecere,* Christopher M. Reilly,[§] Kenneth J. Oestreich,[¶] Stanca M. Ciupe,[†] and Xin M. Luo*

*Department of Biomedical Sciences and Pathobiology, Virginia-Maryland College of Veterinary Medicine, Virginia Polytechnic Institute and State University, Blacksburg, VA; †Department of Mathematics, Virginia Polytechnic Institute and State University, Blacksburg, VA; †Translational Biology Medicine and Health Graduate Program, Virginia Polytechnic Institute and State University, Roanoke, VA; Department of Biomedical Sciences, Edward Via College of Osteopathic Medicine, Blacksburg, VA; and *Department of Microbial Infection and Immunity, Ohio State University College of Medicine, Columbus, OH

ABSTRACT

Aryl hydrocarbon receptor (AhR) responds to endogenous and exogenous ligands as a cytosolic receptor, transcription factor, and E3 ubiquitin ligase. Several studies support an anti-inflammatory effect of AhR activation. However, exposure to the AhR agonist 2,3,7,8-tetrachlorodibenzo-p-dioxin (TCDD) during early stages of development results in an autoimmune phenotype and exacerbates lupus. The effects of TCDD on lupus in adults with pre-existing autoimmunity have not been described. We present novel evidence that AhR stimulation by TCDD alters T cell responses but fails to impact lupus-like disease using an adult mouse model. Interestingly, AhR antagonist CH223191 also changed T cell balance in our model. We next developed a conceptual framework for identifying cellular and molecular factors that contribute to physiological outcomes in lupus and created models that describe cytokine dynamics that were fed into a system of differential equations to predict the kinetics of T follicular helper (Tfh) and regulatory T (Treg) cell populations. The model predicted that Tfh cells expanded to larger values following TCDD exposure compared with vehicle and CH223191. Following the initial elevation, both Tfh and Treg cell populations continuously decayed over time. A function based on the ratio of predicted Treg/Tfh cells showed that Treg cells exceed Tfh cells in all groups, with TCDD and CH223191 showing lower Treg/Tfh cell ratios than the vehicle and that the ratio is relatively constant over time. We conclude that AhR ligands did not induce an anti-inflammatory response to attenuate autoimmunity in adult lupus mice. This study challenges the dogma that TCDD supports an immunosuppressive phenotype. *ImmunoHorizons*, 2024, 8: 172–181.

Received for publication March 29, 2023. Accepted for publication January 16, 2024.

Address correspondence and reprint requests to: Dr. Xin M. Luo or Dr. Stanca M. Ciupe, Department of Biomedical Sciences and Pathobiology, Virginia Polytechnic Institute and State University, Blacksburg, VA 24061 (X.M.L.) or Department of Mathematics, Virginia Polytechnic Institute and State University, Blacksburg, VA 24061 (S.M.C.) E-mail addresses: xinluo@vt.edu (X.M.L.) or stanca@vt.edu (S.M.C.)

ORCIDs: 0000-0002-3756-0322 (F.G.); 0000-0001-5234-2297 (Q.M.M.); 0000-0001-5704-5064 (K.A.R.); 0000-0003-3606-675X (M.R.E.); 0000-0001-9929-7307 (X.C.-P.); 0000-0002-6724-6318 (J.C.T.); 0009-0004-6859-9491 (T.X.); 0000-0001-5015-8170 (R.L.); 0009-0008-6529-0666 (P.A.); 0000-0002-3004-072X (K.J.O.); 0000-0002-5386-6946 (S.M.C.); 0000-0002-2809-5836 (X.M.L.).

This work was supported by Virginia Tech Postbac Research Education Program through National Institutes of Health Training Grant 2R25GM066534-18 (to F.G.), X.M.L. and B.K.S. were supported by National Institutes of Health Grants AR073240 and AT010977, and S.M.C. and Q.M.M. were supported by National Science Foundation Grants 1813011 and 2051820.

F.G., Q.M.M., B.K.S., K.A.R., M.R.E., S.M.C., K.J.O., and X.M.L. contributed to the experimental design; F.G., Q.M.M., B.K.S., M.R.E., L.A., X.C.-P., J.C.T., T.X., and C.M.R. contributed to experimental execution and data collection; F.G., Q.M.M., B.K.S., T.X., R.L., P.A., T.E.C., S.M.C., and X.M.L. performed data analysis and interpretation; and X.M.L., B.K.S., Q.M.M., and S.M.C. wrote and revised the manuscript.

Abbreviations used in this article: AhR, aryl hydrocarbon receptor; ANA, antinuclear Ab; ARNT, AhR nuclear translocator; HAH, halogenated aryl hydrocarbon; SLE, systemic lupus erythematosus; TCDD, 2,3,7,8-tetrachlorodibenzo-*p*-dioxin; Tfh, T follicular helper; Treg, regulatory T.

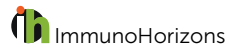
The online version of this article contains supplemental material

This article is distributed under the terms of the CC BY-NC 4.0 Unported license.

Copyright © 2024 The Authors

¹Current address: Pathobiology Graduate Program, Brown University, Providence, RI.

²These authors contributed equally to this work.



INTRODUCTION

Aryl hydrocarbon receptor (AhR) is a promiscuous receptor that binds halogenated aryl hydrocarbons (HAHs), polycyclic aryl hydrocarbons, flavonoids, or endogenously synthesized molecules such as microbially derived tryptophan catabolites (1). 2,3,7,8-Tetrachlorodibenzo-p-dioxin (TCDD) is a prototypical ligand that belongs to the HAH group and is one of the most studied AhR ligands (1). It is formed through combustion of organic, carbon-based material in the presence of chlorine (2). Studies of TCDD exposure in humans indicate an immunosuppressive effect (3, 4); however, this has been a topic of some contention. Corroborating evidence in animals shows that TCDD skews the immune response toward a regulatory T (Treg) cell phenotype that prevents diabetes, mitigate colitis, and suppresses pertussis toxin-induced inflammation (5-8). AhR can bind to the Foxp3 promoter and directly enhance levels of Foxp3 expression (8) as well as reverse colitis-induced methylation of Foxp3 CpG islands (5). TCDD treatment in experimental autoimmune encephalomyelitis attenuated disease pathology (8) and, at a relatively high concentration, induced a regulatory phenotype in human T cells (9). Even though it is a toxin processed by the liver, TCDD can also suppress hepatic injury 5 d after administration by increasing serum TGF-β level and mobilizing migration of myeloid-derived suppressor cells to the peritoneal cavity (10). Furthermore, AhR stimulation shifted the phenotype of ex vivo macrophages from systemic lupus erythematosus (SLE) patients toward an M2 state (11). Taken together, these studies provide evidence on the anti-inflammatory action of AhR stimulation that presents the potential to be harnessed therapeutically.

The canonical signaling pathway for AhR is stimulated by TCDD (1). Intracellular ligand binding dissociates AhR from a cytosolic sequestering protein complex and allows for entry into the nucleus (1). In the nucleus, AhR binds to AhR nuclear translocator (ARNT) and recognizes a 5'-GCGTC-3' motif known as a dioxin response element, which is found on many genes including the canonically transcribed genes Cyp1A1, Il22, and Ahrr (1, 12). Noncanonically, AhR has been found to bind partners such as the NF-κB-associated protein RELB, promoting *Tnsfs13b* transcription (1), or RORyt in the cytosol independent of ligands, promoting Il17 transcription and a Th17 phenotype (13). AhR functions not only as a transcription factor, but it is also an E3 ubiquitin ligase that regulates levels of many proteins including ERa through interaction with the Cul4B ubiquitin ligase complex (14-17). Curiously, some compounds that partially inhibit transcriptional activity dock the AhR Per/Arnt/Sim ligand binding pocket and induce E3 ubiquitin ligase activity independently of ligands (14, 17, 18). One antagonist with selective inhibition of HAH-induced transcriptional activity, CH223191, similarly enters the ligand binding pocket to inhibit agonist-activated transcription, but the activation of the ubiquitin ligase complex by this compound has not yet been determined (19, 20).

Toning of the AhR signal by different ligand classes is evidenced by the differential effects on the immune system (1, 8, 21, 22). While the mechanism is incompletely understood,

some have proposed that this may be due to the effects of ligand affinity and concentration. Some studies have, in fact, shown dose-dependent effects on T cells (23, 24). Additionally, strainand species-specific variations in AhR protein affinity for ligand have been observed (25, 26). Variations in mice are due to single residue differences in the C-terminal ligand-binding domain. Two allelic variants have been identified in mice, the AhR^b (A357) variant has ~10-fold higher sensitivity to ligands compared with the AhR^d (V357) (26). MRL/lpr and DBA mice have the AhR^d variant, whereas C57BL/6 and C3H/lpr mice have the high-affinity AhRb variant (25, 26). The human AHR allele similarly has a 10-fold reduction in affinity compared with the AhR^b variant; however, mutating the corresponding valine residue (V381) to an alanine does not increase affinity for ligand (23). Prior studies have shown that TCDD exposure prenatally in C57BL/6 mice induces an autoimmune phenotype (27, 28), and that prenatal exposure in SNF1 lupus mice exacerbates autoimmunity (29). How TCDD affects adult lupus mice, however, was unknown. Notably, Gogal and colleagues (29) used a dose of 5 µg/kg in C57BL/6 mice (27, 28), and in the SNF1 mice, which have the low-affinity AhRd variant, they used a dose \sim 10-fold higher. Given the similarity in affinity between the human AhR protein and the MRL/lpr variant, we decided to use the MRL/lpr lupus-prone mouse model to investigate the effects of TCDD on autoimmunity. However, we decided against using the 10-fold dose, because even a low body burden of 100 ng of TCDD per kilogram of body weight led to severe adverse effects in people following accidental exposure (30). Instead, we chose a lower dose of 10 µg/kg. We found no evidence that this dose of TCDD exerted any immunosuppressive effect, as it did not alter levels of TGF-β. However, it induced T follicular helper (Tfh) cells and altered the ratio of Tfh to Treg cells. Therefore, we concluded that this dose of TCDD altered T cell balance in adult lupus-prone mice. An HAH transcriptional antagonist, CH223191, in contrast, downregulated Treg cells in our mouse model.

MATERIALS AND METHODS

Mice

Female MRL/lpr mice were generated in-house with breeders purchased from The Jackson Laboratory (Bar Harbor, ME). Mice were housed under specific pathogen-free conditions at Virginia Polytechnic Institute and State University (Blacksburg, VA). At 8 and 10 wk of age mice were injected i.p. with 50 μ l of vehicle corn oil (Sigma-Aldrich), 10 μ g/kg TCDD (Toronto Research Chemicals), or 10 mg/kg CH223191 (Sigma-Aldrich). Five days after each injection, blood was collected by retroorbital bleeding. Mice were sacrificed at 15 wk of age and tissues were harvested for analysis.

Promoter reporter assay

The full mouse Tgfb1 promoter (-1162 to +764 bp) was generated by Invitrogen GeneArt services and ligated into the pGL3-pro



luciferase reporter construct (Promega). The Ahr^b coding sequence was cloned into to pcDNA3.1/V5-His-TOPO vector (Thermo Fisher Scientific) from C57BL/6 derived in vitro differentiated T_h 17 cDNA. Primers used for cloning and validation are available upon request. HEK-239T cells (provided by the laboratory of Dr. James Smyth) were cultured using the American Type Culture Collection recommendation to \sim 70% confluency and cotransfected with promoter reporter, overexpression, and SV40-Renilla (Promega) vectors using an optimized concentration of Lipofectamine 2000 reagent (Thermo Fisher Scientific). Cells were incubated posttransfection for 2 d at 37°C, 5% CO₂. The Dual-Glo luciferase assay (Promega) was performed and luciferase was measured with SpectraMax M5. Luciferase expression was normalized to the internal Renilla control.

RNA extraction, reverse transcription, and quantitative PCR

Spleen tissue was snap-frozen in liquid nitrogen and stored at -80° C. Tissue was processed with a sterilized mortar and pestle and a Bullet Blender tissue homogenizer. RNA extraction was performed using an RNeasy Plus universal kit (Qiagen). cDNA was synthesized using iScript reverse transcription supermix (Bio-Rad). Quantitative PCR was performed using Fast SYBR Green master mix (Thermo Fisher Scientific) and an Applied Biosystems 7500 Fast system. Relative quantities of transcripts were calculated using the $2^{-\Delta\Delta Ct}$ method after being normalized to the *18S rRNA* housekeeping gene. Already validated primer sequences were obtained from the Harvard PrimerBank: *Tgfb1*, forward 5'-CCA CCT GCA AGA CCA TCG AC-3', reverse 5'-TCG AGT GAC AAA CAC GAC TGC-3'; *Il22*, forward 5'-ATG AGT TTT TCC CTT ATG GGG AC-3', reverse 5'-GCT GGA AGT TGG ACA CCT CAA-3'.

Cell preparation and flow cytometry

Splenic lymphocytes were isolated by homogenizing fresh tissue on a 70-μm strainer and incubated with 1× RBC lysis buffer (eBioscience). Cells were stained with surface markers, fixed, and stained intracellularly using Foxp3/transcription factor staining buffer set (eBioscience). CD3⁺ T cells were stained using PD1-FITC, CXCR5-PE, CD8-PerCP-Cy5.5, CD4-allophycocyanin, Foxp3-BV421, live-dead Zombie Aqua (BioLegend). Flow cytometry was performed using a FACSAria fusion cell sorter (BD Biosciences).

Cytokine and autoantibody expression

Serum cytokine and autoantibody levels were measured using ELISA or Luminex FLEXMAP 3D. TGF- β was measured using a TGF- β 1 human/mouse ELISA Ready-SET-Go! kit (eBioscience). IL-22 was measured using a commercial kit (Thermo Fisher Scientific). Anti-dsDNA IgG autoantibodies were measured as previously described (31).

Renal histopathology

Tissues were paraffin embedded, sectioned, and stained for periodic acid–Schiff at the Histopathology Laboratory at the Virginia-Maryland College of Veterinary Medicine. Glomerular lesions were graded on a scale of 0–3 for increased cellularity, increased mesangial matrix, necrosis, percentage of sclerotic glomeruli, and presence of crescents. Similarly, tubulointerstitial lesions were graded on a scale of 0–3 for interstitial mononuclear infiltration, tubular damage, interstitial fibrosis, and vasculitis. Slides were scored by a board-certified veterinary pathologist (T.E.C.) in a blinded fashion.

Antinuclear Ab measurement

The assessment of antinuclear Abs (ANAs) in the mouse serum was carried out using a HEp-2 cells ANA kit (Antibodies, Inc.) following the manufacturer's procedures. Images were captured with a Zeiss LSM 880 confocal microscope. Image processing and quantification of the mean fluorescence intensity were performed with ZEN 2.1 Lite software. Analysis of the ANA pattern expression was performed in a blinded fashion (R.L./P.A.) using the ImageJ software. We defined each pattern according to the demonstration from the ANA testing kit. Four different patterns were characterized as follows: peripheral, homogeneous, cytoplasmic spider web, and fine speckled. Each pattern was given an arbitrary number and counted utilizing the particle tracking function of ImageJ software.

Statistical analysis

For quantitative PCR, $\Delta\Delta$ Ct analysis was performed using 18S rDNA as a housekeeping control. Data were analyzed with GraphPad Prism and graphs display mean \pm SEM. Normality of data distribution was determined. Statistical significance for comparison of means was determined in normally distributed data by a one- or two-way ANOVA and a Tukey post hoc test. A p value <0.05 was considered statistically significant.

Mathematical modeling

To determine the kinetics of Tfh and Treg cell populations after injection with TCDD or CH223191, we developed mathematical models describing the interaction between Tfh cells, Treg cells, four cytokines, and anti-dsDNA Ab for which experimental data were collected at 8, 10, and 15 wk of age (T0, T2, and T7). We assumed that the dynamics of the anti-dsDNA Ab (A) and two cytokine populations, IL-6 (I_6), and TGF- β (F_β), can be described by the function

$$w(t) = a_w e^{b_w t}, (1A)$$

where a_w is the population value at time T0, b_w is the population growth rate, and $w = \{A, I_6, F_\beta\}$. We fitted w(t) to averages of population levels at times T0, T2, and T7 using the "fit" algorithm in MATLAB. The estimates for parameters a_w and b_w are presented in Supplemental Table I, and the resulting dynamics and data are shown in Fig. 4A. Similarly, we assumed that the



dynamics of the remaining cytokine populations IL-2 (I_2) and IL-12 (I_{12}) can be described by the function

$$w(t) = x_w t^2 + y_w t + z_w, (1B)$$

where x_w , y_w , and z_w are arbitrary numbers and $w = \{I_2, I_{12}\}$. We fit these polynomials to the average mean florescence intensity data for I_2 and I_{12} using the polyfit function in MATLAB. The estimates for parameters x_w , y_w , and z_w are presented in Supplemental Table II, and the resulting dynamics and data are shown in Fig. 4.

Lastly, the cell populations Tfh (T_{fh}) and Tr (T_r) are given by a two-order nonlinear system of ordinary differential equations

$$\frac{dT_{fh}}{dt} = \frac{s_{T_{fh}}I_{12}}{k_{T_{fh}} + I_2} - d_{T_{fh}}T_{fh},
\frac{dT_r}{dt} = \frac{s_{T_r}F_{\beta}}{k_{T_r} + I_2 + I_6} - d_{T_r}T_r,$$
(1C)

where s_w accounts for population production, d_w accounts for per capita death rate, k_w accounts for population densities where production is half-maximal, and $w = \{T_{fh}, T_r\}$. We assume that the T_{fh} production is enhanced by I_{12} and inhibited in the presence of I_2 (see Fig. 5A). Similarly, the T_r production is enhanced by F_β and inhibited by I_2 and I_6 (see Fig. 5A). We used the following values to parametrize the model. The decay rates per week were computed as $d_w = 7\ln(2/t_{1/2})$, where the $t_{1/2}$ for each population, w, is known from literature. The T_{fh} and T_r values at day T7 are known (Supplemental Table III). We fixed s_w and k_w to arbitrary rates (Supplemental Table III) and used the model (Eq. 1C) with all of the cytokine values over time known from data fitting (Fig. 4) to determine the values of T_{fh} and T_r at time T0 (Supplemental Table III), as well as temporal solutions for populations T_{fh} and T_r (Fig. 5B, 5C).

RESULTS

TCDD induces TGF-β via the AhR signaling pathway

Based on evidence for the immunosuppressive effect of TCDD and increases in TGF-β in mouse models, we hypothesized that TCDD would suppress autoimmune disease. TGF-β is a known downstream target of AhR that reciprocally affects AhR expression (1). Notably, the Tgfb1 promoter contains two dioxin response elements (Supplemental Fig. 1A). We cloned the full mouse Tgfb1 promoter and the mouse Ahr^b coding sequence from C57BL/6 mice. Both Ahrb overexpression (EmAhR) and a Tgfb1 promoter reporter construct (PRmTGF-b1) were required in HEK293T cells with TCDD stimulation to induce luciferase activity (Supplemental Fig. 1B). Luciferase activity was not increased in the absence of mouse AhR overexpression. Furthermore, stimulation of mouse AhR alone was sufficient, and a mouse ARNT counterpart was not necessary. Although we did not test the low-affinity mouse Ahr^d coding sequence from MRL/lpr mice, we hypothesized that TCDD would still induce TGF- β in the presence of Ahr^d, albeit a higher concentration of TCDD might be required. We decided

to move on to in vivo investigation of the effects of TCDD as well as an HAH transcriptional antagonist, CH223191, on disease phenotype and pathogenesis of lupus in MRL/lpr mice.

TCDD and CH223191 do not significantly alter TGF- β or impact lupus-like disease in the MRL/ β pr mouse model

MRL/lpr mice were injected i.p. with TCDD or the HAH transcriptional antagonist CH223191 (Fig. 1A) at 8 and 10 wk of age, and blood serum was collected 5 d after each injection (TO and T2, respectively). Mice were sacrificed at 15 wk of age (T7). No significant differences were found in TGF-β expression in TCDD-treated or CH223191-treated mice at any time point (Fig. 1B). No significant difference in Tgfb1 splenic mRNA transcription was observed, either (Fig. 1C). Body weights were consistent between groups throughout the study (data not shown), and neither the spleen weights (Fig. 1D) nor the levels of circulating anti-dsDNA IgG Abs (Fig. 1E) were significantly different among groups. Therefore, the hypothesis for induction of an ameliorative effect by TCDD-induced TGF-β was not supported. Notably, we are confident that these mice had developed lupuslike disease, as the anti-dsDNA IgG levels were significantly higher at T7 compared with T0 (Fig. 1E, p < 0.05).

To confirm activity of TCDD and CH223191 in the absence of anticipated phenomena, activation of the AhR pathway was evaluated by measuring splenic mRNA levels of both canonical and noncanonical AhR transcriptional activity at T7. TCDD has a $t_{1/2}$ of 8 d in mice (32), and it is therefore not surprising that splenic mRNA levels of Ahr and Cyp1a1 are not significantly altered in the treatment groups at T7 (data not shown). However, whereas the protein level of IL-22 was suppressed by TCDD at both time points (Supplemental Fig. 1C), Il22 mRNA levels were significantly elevated by TCDD and CH223191 (Fig. 1F), suggesting that both exposures induced the transcription of this cytokine. Thus, signaling through AhR was indeed activated by TCDD, and, given that TCDD and CH223191 had similar effects on Il22 mRNA levels, there may be nontranscriptionally related effects of AhR stimulated by both TCDD and CH223191. We concluded that the lack of TGF-β induction was not due to an absence of stimulation by the respective compounds selected for this study. Indeed, there was a trending increase of proteinuria with TCDD, as well as significant aggravation of proteinuria at 12 wk of age with CH223191 (Fig. 1G), although at the time of euthanasia the renal histopathology was no longer different among the three groups (Supplemental Fig. 1D). At the age of 15 wk, the weights of superficial lymph nodes (axillary and cervical) were elevated with TCDD and CH223191 (Fig. 1H), again suggesting that the treatments were effective at exacerbating lupus-like disease. No differences were observed in deep lymph nodes weights (i.e., mesenteric or renal; data not shown).

Consistently, we observed serum ANA patterns on HEp-2 cells that may have indicated more severe disease with TCDD and CH223191 (Fig. 2A). CH223191, specifically, induced a peripheral ANA pattern indicative of acute lupus-like disease at both T2 and T7 time points (Fig. 2B), whereas TCDD and



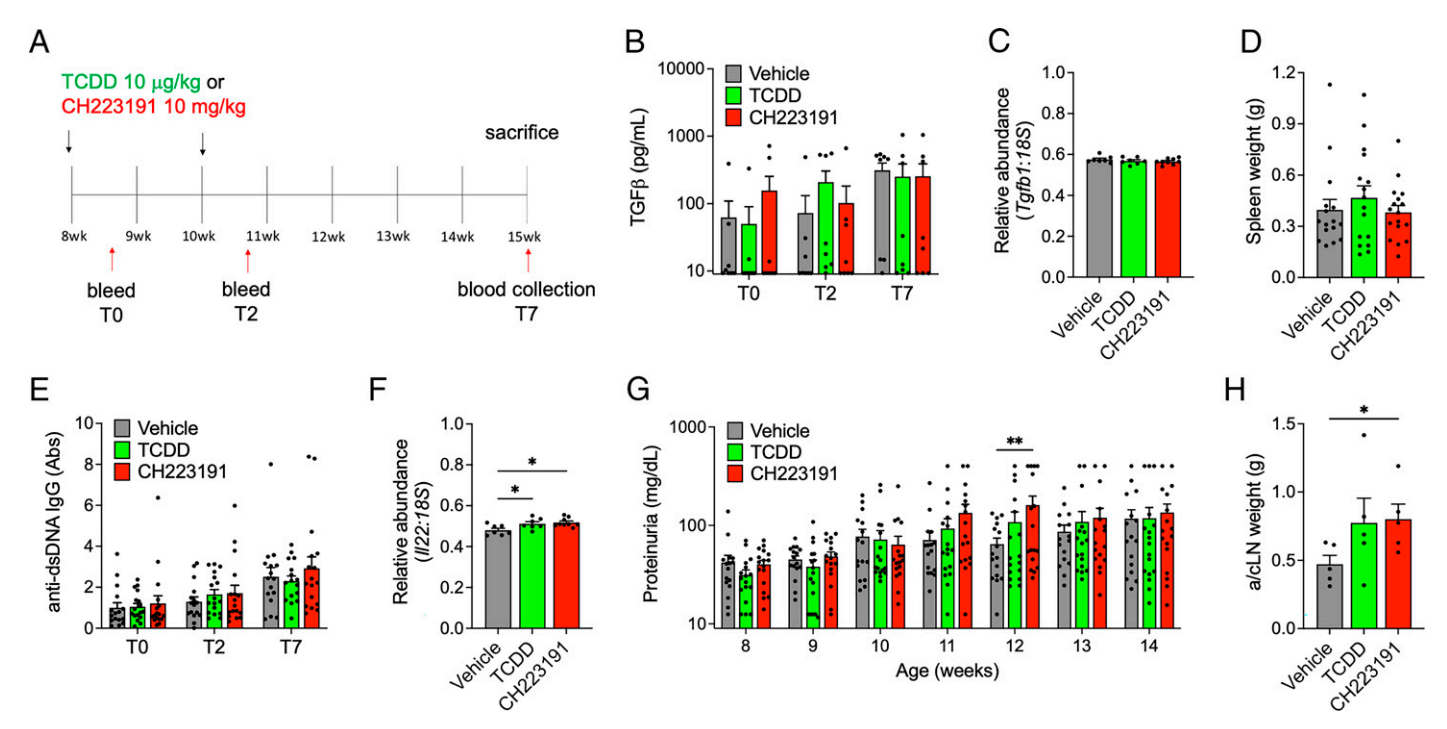


FIGURE 1. TCDD and CH223191 do not significantly alter TGF- β or impact lupus-like disease in the MRL/lpr mouse model.

(A) MRL/lpr mice received vehicle, $10 \mu g/kg$ TCDD, or 10 mg/kg CH233191 according to the diagram of experimental design. The same experiment was repeated once, with n = 8-9/group in each experiment. (B) Serum TGF- β at T0, T2, and T7. (C) T7 splenic *Tgfb1* transcript level. (D) T7 spleen weight. (E) Level of anti-dsDNA lgG autoantibodies at T0, T2, and T7. (F) T7 splenic *Il22* transcript level. *p < 0.05 by one-way ANOVA. (G) Proteinuria from 8 to 14 wk of age. **p < 0.01 by two-way ANOVA. (H) Weights of superficial (axillary and cervical) lymph nodes at T7. Only one cage per group (n = 5/group) was analyzed for this parameter. *p < 0.05 based on one-way ANOVA. For (D), (E), and (G), data from both experiments were combined.

CH223191 induced a cytoplasmic spider web pattern on HEp-2 cells at T7, suggesting the presence of autoantibodies against cellular structural Ags such as actin and myosin (Fig. 2B). However, only the ANA patterns, but not the overall fluorescence intensity (Supplemental Fig. 1E), were changed by the treatments. This suggests that TCDD and CH223191 may have impacted lupus, but the effects are minimal.

Based on these results, the hypothesis that TCDD and CH223191 failed to induce an anti-inflammatory response to attenuate the autoimmune disease is supported. In fact, CH223191 significantly aggravated glomerulonephritis (indicated by increased proteinuria at 12 wk) and deteriorated lymphadenopathy (indicated by increased superficial lymph node weights at T7) in MRL/lpr mice. This suggests that TCDD may not affect

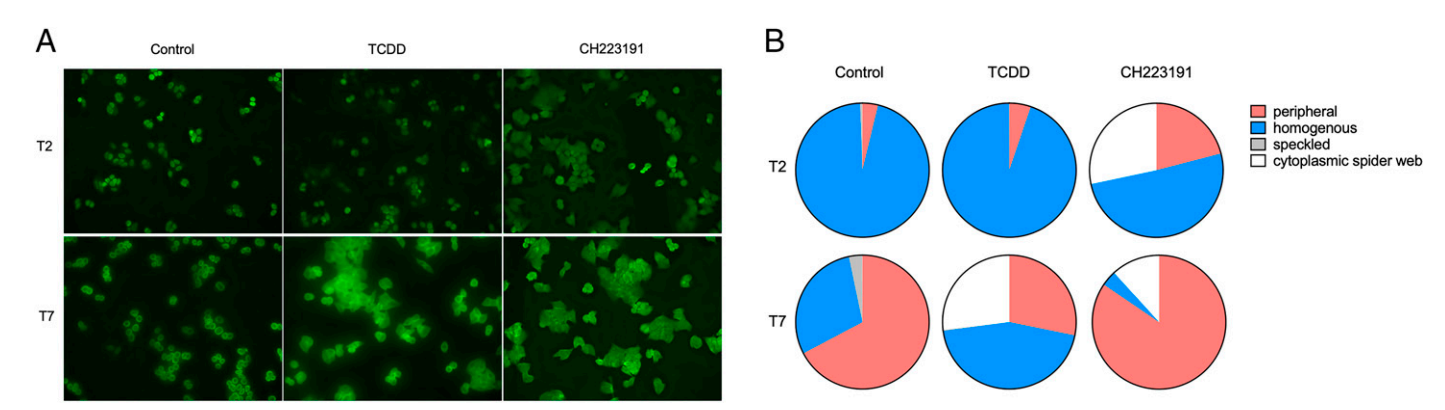


FIGURE 2. TCDD and CH223191 alter serum ANA patterns on HEp-2 cells.

(A) Representative images. (B) Pie charts showing the proportions of different ANA patterns. The peripheral pattern is indicative of acute SLE-like disease. The homogeneous pattern is the most typical of SLE. Both peripheral and homogeneous patterns indicate autoantibodies against dsDNA and histones. The speckled pattern, which is rare in SLE, usually indicates autoantibodies against mitochondria. The cytoplasmic spider webs suggest autoantibodies against structural Ags such as actin and myosin.



autoimmunity through its HAH activity. Furthermore, our data indicate that both TCDD and CH223191 altered the serum ANA patterns on HEp-2 cells, again suggesting that the treatments were effective but failed to modulate lupus-like disease in MRL/lpr mice.

TCDD and CH223191 impact Tfh and Treg cells, respectively

The exacerbation of glomerulonephritis and lymphadenopathy by TCDD and CH223191 suggested that the immune response might be aggravated by both exposures. To search for evidence, we decided to explore cell-mediated responses including CD4⁺ CXCR5⁺PD-1⁺ follicular Tfh cells and CD4⁺Foxp3⁺ Treg cells. As anticipated, splenic Tfh cells were significantly increased by TCDD (Fig. 3A), whereas splenic Treg cells were significantly reduced by CH223191 (Fig. 3B), leading to the Tfh/Treg cell balance skewing toward Tfh cells by both treatments (Fig. 3C). CD8⁺Foxp3⁺ T cells, also known as suppressor T cells, are similar to their CD4⁺ counterparts with a more limited capacity for suppressing the immune response (33, 34). The effect on Foxp3 levels was indiscriminate of T cell phenotype, and CD8⁺ Foxp3⁺ cells were significantly reduced by both TCDD and CH223191 (data not shown). These results suggest that TCDD and CH223191 promote follicular T cell response while reducing the suppressive arm of immunity in MRL/lpr mice.

Modeling lupus pathology reveals dynamics of cellular expansion and contraction

To determine the kinetics of Tfh and Treg populations after injection with TCDD or CH223191, we developed mathematical

models describing the interaction between Tfh cells, Treg cells, four cytokines, and anti-dsDNA Ab for which experimental data were collected at 8, 10, and 15 wk of age (T0, T2, and T7). We assumed that the dynamics of the anti-dsDNA Ab (A) and two cytokine populations IL-6 (I_6) and TGF- β (F_β) can be described by the function $w(t) = ae^{bt}$ (see Materials and Methods, Eq. 1A) for details), where a is the population value at time T0 and b is the population growth rate. We fitted w(t) to averages of population levels at times T0, T2, and T7. The estimates for parameters a and b are presented in Supplemental Table I, and the resulting dynamics and data are shown in Fig. 4A. Similarly, we assumed that the dynamics of the remaining cytokine populations IL-2 (I_2) and IL-12 (I_{12}) can be described by function $w(t) = xt^2 + yt + z$ (see Materials and Methods and Eq. 1B for details). We fitted w(t) to averages of population levels at times T0, T2, and T7. The estimates for parameters x, y, and z are presented in Supplemental Table II, and the resulting dynamics and data are shown in Fig. 4. Although the vehicle treatment generally increased the cytokine levels over time, indicative of disease progression, with the exception of IL-12 (Fig. 4A), with TCDD and CH223191 treatments, IL-6 stayed relatively constant, whereas IL-12 decreased at the later time point (Fig. 4B, 4C). Lastly, we developed a deterministic ordinary differential equation model for the interaction between two cell populations, Tfh (T_{fb}) and Treg (T_r) , and the cytokine populations described above (Equation 1C, Fig. 5A). Rates of Tfh and Treg cell decay were used from experimental evidence found in the literature $(t_{1/2} \text{ of } 7-11 \text{ d}; \text{ lifespan of } 14-22 \text{ d}), \text{ and } \text{Tfh and } \text{Treg cell rates}$ at time T7 were found experimentally. To determine the Tfh

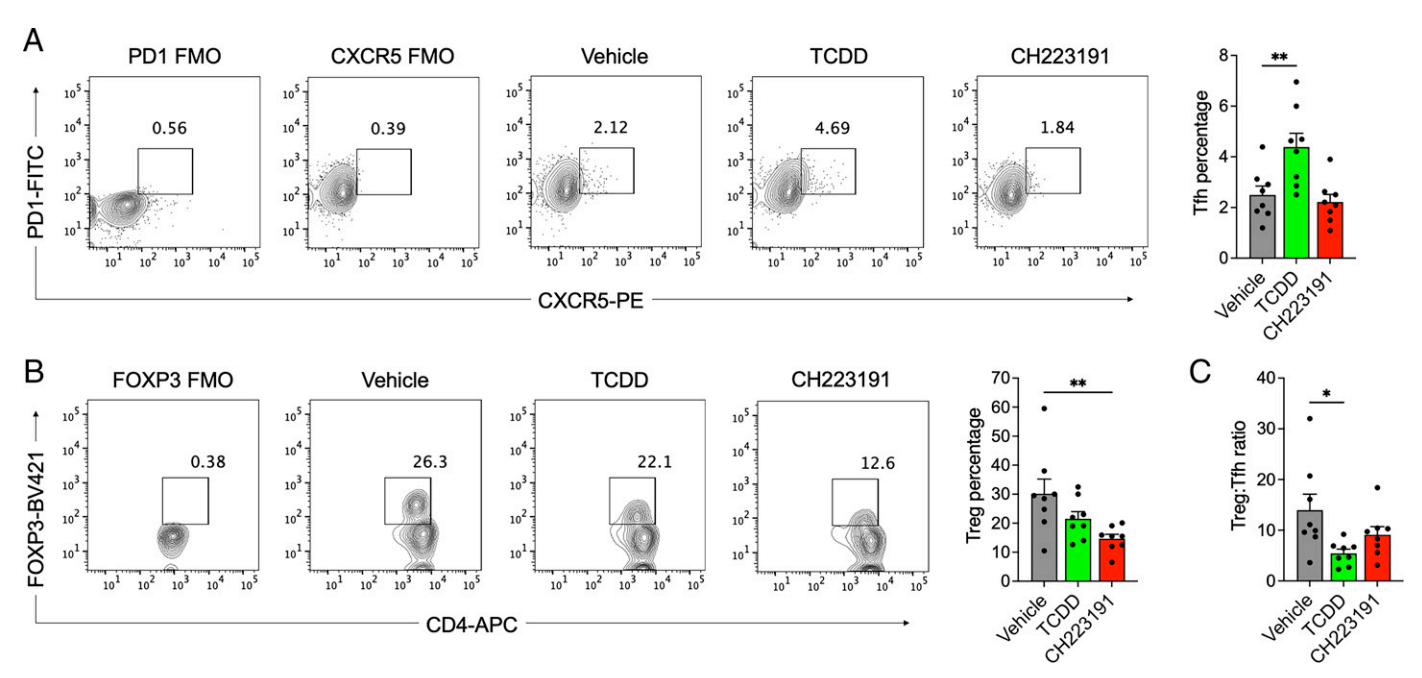


FIGURE 3. TCDD and CH223191 impact Tfh and Treg cells, respectively.

(A) Representative FACS plots and percentage of Tfh cells within CD4⁺ T cells in the T7 spleen. **p < 0.01 by one-way ANOVA. FMO, fluorescence minus one. (B) Representative FACS plots and percentage of Treg cells within CD4⁺ T cells in the T7 spleen. **p < 0.01 by one-way ANOVA. (C) Ratio of Treg to Tfh cells in the T7 spleen. *p < 0.05 by one-way ANOVA. Data from one representative experiment are shown (n = 8/group).



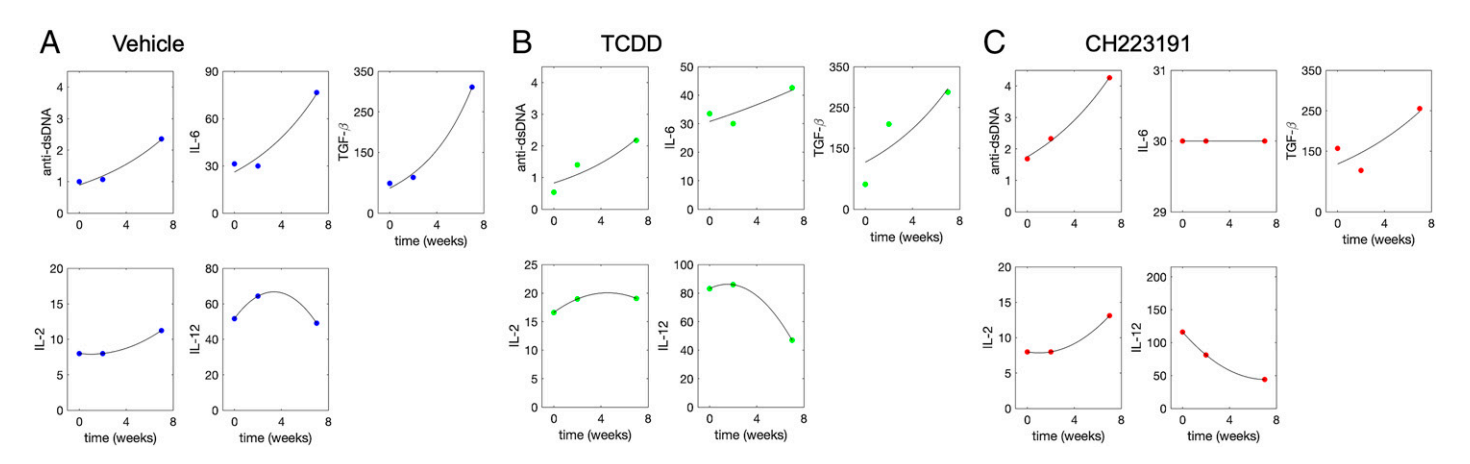


FIGURE 4. Predicted population dynamics over time versus data.

Theoretical curves (black lines) obtained by fitting solutions of the form $w(t) = ae^{bt}$ for populations $w = \{A, I_6, F_\beta\}$ and of the form $w(t) = xt^2 + yt + z$ for populations $w = \{I_2, I_{12}\}$ to time series data for experimental groups. (A) Vehicle (blue points). (B) TCDD (green points). (C) CH223191 (red points). Parameters estimates are listed in Supplemental Tables I and II. The x-axis represents weeks postinjection with T0, T2, and T7 representing 8, 10, and 15 wk since birth, respectively. For the Ab populations (anti-dsDNA) the y-axis represents the averaged normalized absorbance. For cytokine populations, the y-axis represents the average (pg/ml).

and Treg values at time T0, we ran the differential equation model (Eq. 1C) backward (Fig. 5B, 5C, Supplemental Table III). The resulting predictions showed that at time T0, 5 d after the first injection, Tfh populations were expanded most highly in the TCDD-treated group (Fig. 5B) and the level decreased slightly by time T7. Tfh population levels for the vehicle and CH223191-treated groups remained nearly identical from T0 to T7. Both Tfh and Treg cell populations decayed continuously in all groups (Fig. 5B). Treg levels exceeded Tfh levels in all groups for the duration of the experiment, with the vehicle group having the largest Treg/Tfh cell ratio throughout the study and the Treg/Tfh cell ratio having remained consistently lower in the TCDD and CH223191 groups compared with the vehicle (Fig. 5C). The results corroborate the evidence for expansion of the follicular T cell response in TCDD-treated mice, and that the contraction of Treg cells occurs regardless of treatment.

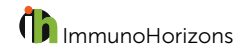
Overall, we found no evidence to support the suppressive effects of TCDD in a model of adult lupus. Instead, TCDD causes alteration of follicular homeostasis, reducing immunosuppressive cell phenotypes and promoting follicular phenotype formation. Interestingly, we found that the antagonist CH223191 did not have an opposite effect on the immune system. In some cases, such as *Il22* mRNA levels and Foxp3⁺ cell populations, it caused a similar phenotype to TCDD exposure that might signify disease exacerbation.

DISCUSSION

Recent studies have revealed an anti-inflammatory role for AhR activation in both autoimmune and infection models, where the lack of AhR signaling led to exacerbated lupus and increased Tfh cells, respectively (35, 36). We found that TCDD exposure in an SLE mouse model with similar AhR affinity compared

with humans failed to induce anti-inflammatory effects; instead, it reduced immunosuppressive cell phenotypes and prompted follicular phenotype formation. The findings are congruent with other reports of AhR ligands exacerbating autoimmune disease. Endogenous synthesis of AhR ligands by the skin in response to UV light has been shown to exacerbate skin rashes and lesions in lupus erythematosus (37). Environmental pollutants also contribute to autoimmunity, and, notably, autoimmunity-linked air pollutants affect the immune system through AhR, such as crystalline silica and fine particulate matter (PM2.5) (38). However, most studies linking TCDD to autoimmunity exacerbation pertain to the effects during early stages of development (27–29). Therefore, evidence exposing how TCDD affects autoimmunity in adult mice with a similar AhR ligand affinity to humans is key to therapeutically harnessing AhR anti-inflammatory potential.

One interesting finding was the destabilization of Foxp3⁺ cell populations. A relative of AhR in the bHLH family, HIF-1α, is known to regulate Foxp3 protein stability by direct binding with its bHLH domain to the C terminus of Foxp3 and subsequent targeting for degradation by ubiquitin ligation by the von Hippl-Lindau protein-associated proteasome (39). AhR is a ligand-dependent E3 ubiquitin ligase in the bHLH family, and AhR antagonists that prevent transcriptional activity by binding to the ligand pocket also induce E3 ubiquitination and degradation (14-17). We considered that TCDD and CH223191 may have similar effects on Foxp3 by promoting protein degradation through AhR's E3 ubiquitin ligase activity. Indeed, Xiong et al. (40) recently found that Foxp3 binds AhR at either the bHLH or Per/Arnt/Sim domain to enhance Gpr15 transcription. The evidence for direct binding of AhR-Foxp3 makes a compelling argument for the ability of AhR E3 ubiquitin ligase activity to regulate levels of Foxp3 protein. Foxp3 is the master transcriptional factor for Treg cells. Treg cells are identified as critical



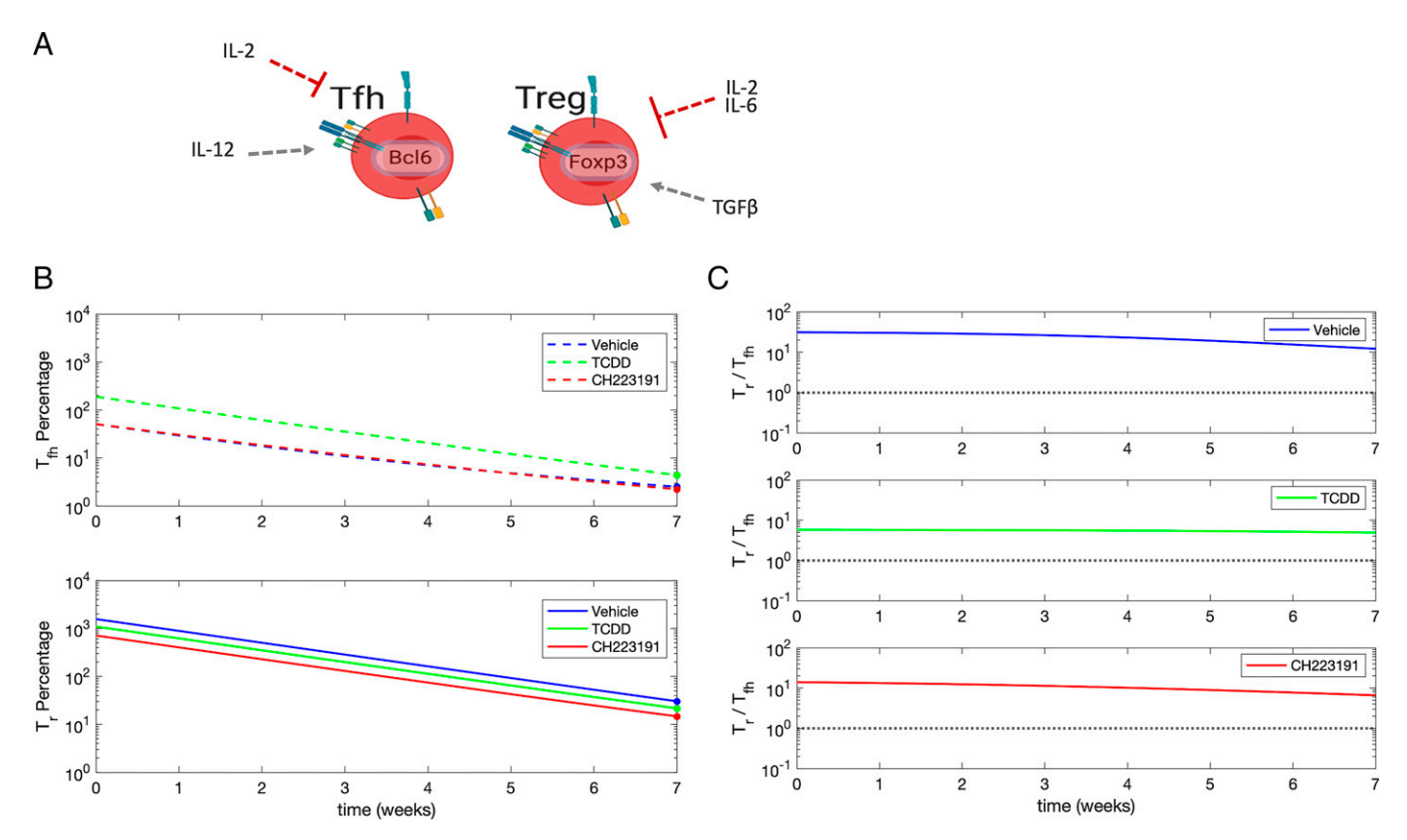


FIGURE 5. Dynamics of Tfh and Treg population over time.

(A) Model diagram of cytokine interactions with Tfh and Treg cell populations. (B) Logarithmic dynamics of percentage of Tfh (top) and Treg (bottom) cells within CD4 $^+$ T cells from T0 to T7 obtained by evaluating model (Eq. 1C). Parameters are given in Supplemental Table III. (C) Logarithmic dynamics of Treg/Tfh cell ratio given by evaluating model (Eq. 1C) from T0 to T7. Dotted lines correspond to Tr/Tfh = 1. Parameters are given in Supplemental Table III.

regulators of autoimmunity, and the loss of the Treg cell phenotype by TCDD and CH223191 may contribute to the slightly aggravated symptoms of nephritis and lymphadenopathy. The contradiction with most studies indicating that TCDD promotes Treg cells may be resolved by examining the cross-section of allelic variations in AhR affinity for ligands and dose-dependent effects of TCDD. It is also possible that the molecular control for transcriptional activity versus E3 ubiquitin ligase activity is concentration- and affinity-dependent. Furthermore, we can draw a comparison between the dynamic interactions between HIF- 1α and the E3 ubiquitin ligase von Hippl-Lindau in both the degradation and maintenance of the Foxp3⁺ Treg cell phenotype (39, 41).

Another interesting finding was that *Il22* transcription was increased 7 wk after initial exposure in both TCDD-and CH223191-treated mice. This is interesting first because *Il22* is considered to be a transcriptional consequence of the canonical signaling pathway, yet the antagonist CH223191 induced the phenotype to the same level as TCDD. Indeed, it is counterintuitive that the agonist and antagonist yielded a similar outcome. Many so-called antagonists are also considered to have agonistic capacities, such 2,3-dimethylindole (18), so it is not surprising

that there are some similarities between TCDD and CH223191. Second, despite being recognized as generally anti-inflammatory, the increased production of IL-22 may have detrimental consequences for autoimmune disease. Patients stratified by active SLE with defective TGF- β signaling were observed to overexpress IL-22, in which AhR signaling has been implicated (42). Similar to TGF- β and IL-10, IL-22 may have contextual beneficial or pathological consequences in autoimmunity (43).

Overall, our study evidences previously unappreciated immunological consequences of AhR activation. We contributed to building a basis of rationale for the design of studies and therapeutics using AhR by characterizing the effects of an otherwise anti-inflammatory inducing dose of TCDD on an AhR^d lupusprone mouse model. We have also developed a (to our knowledge) novel mathematical model that used temporal cytokine data to quantify the Treg/Tfh cell data over time and predicted that Treg cells exceeded Tfh cells in all groups, with TCDD group having the highest Tfh expansion and the lowest Treg/Tfh cell ratio, followed by CH223191 and vehicle, respectively. The model can predict the parameters and mechanisms of SLE severity, which may be applied in future scenarios. Notably, our study used only one lupus mouse model, one agonist, and one



antagonist. Therefore, the findings could be limited to the mouse model and/or the individual agonist/antagonist used. Nonetheless, our study suggests that, moving forward into therapeutic applications of AhR ligands, it is important to recognize the finesse involved in its molecular mechanisms so as to avoid the detrimental impact that AhR pathways have on autoimmunity.

DISCLOSURES

The authors have no financial conflicts of interest.

ACKNOWLEDGMENTS

We thank Dr. James Smyth and Carissa James for the contribution of critical reagents, and the Flow Cytometry Laboratory manager, Melissa Makris, for performing flow cytometry.

REFERENCES

- Lamas, B., J. M. Natividad, and H. Sokol. 2018. Aryl hydrocarbon receptor and intestinal immunity. *Mucosal Immunol*. 11: 1024–1038.
- 2. Von Burg, R. 1988. TCDD. J. Appl. Toxicol. 8: 145-148.
- Tonn, T., C. Esser, E. M. Schneider, W. Steinmann-Steiner-Haldenstätt, and E. Gleichmann. 1996. Persistence of decreased T-helper cell function in industrial workers 20 years after exposure to 2,3,7,8-tetrachlorodibenzo-p-dioxin. Environ. Health Perspect. 104: 422–426.
- Saberi Hosnijeh, F., L. Portengen, H. B. Bueno-de-Mesquita, D. Heederik, and R. Vermeulen. 2013. Circulating soluble CD27 and CD30 in workers exposed to 2,3,7,8-tetrachlorodibenzo-p-dioxin (TCDD). Cancer Epidemiol. Biomarkers Prev. 22: 2420–2424.
- Singh, N. P., U. P. Singh, B. Singh, R. L. Price, M. Nagarkatti, and P. S. Nagarkatti. 2011. Activation of aryl hydrocarbon receptor (AhR) leads to reciprocal epigenetic regulation of FoxP3 and IL-17 expression and amelioration of experimental colitis. *PLoS One*. 6: e23522.
- Kerkvliet, N. I., L. B. Steppan, W. Vorachek, S. Oda, D. Farrer, C. P. Wong, D. Pham, and D. V. Mourich. 2009. Activation of aryl hydrocarbon receptor by TCDD prevents diabetes in NOD mice and increases Foxp3⁺ T cells in pancreatic lymph nodes. *Immunotherapy* 1: 539–547
- Al-Ghezi, Z. Z., N. Singh, P. Mehrpouya-Bahrami, P. B. Busbee, M. Nagarkatti, and P. S. Nagarkatti. 2019. AhR activation by TCDD (2,3,7,8-tetrachlorodibenzo-p-dioxin) attenuates pertussis toxin-induced inflammatory responses by differential regulation of Tregs and Th17 cells through specific targeting by microRNA. Front. Microbiol. 10: 2349.
- 8. Quintana, F. J., A. S. Basso, A. H. Iglesias, T. Korn, M. F. Farez, E. Bettelli, M. Caccamo, M. Oukka, and H. L. Weiner. 2008. Control of $T_{\rm reg}$ and $T_{\rm H}$ 17 cell differentiation by the aryl hydrocarbon receptor. *Nature* 453: 65–71.
- Gandhi, R., D. Kumar, E. J. Burns, M. Nadeau, B. Dake, A. Laroni, D. Kozoriz, H. L. Weiner, and F. J. Quintana. 2010. Activation of the aryl hydrocarbon receptor induces human type 1 regulatory T cell-like and Foxp3⁺ regulatory T cells. *Nat. Immunol.* 11: 846–853.
- Neamah, W. H., N. P. Singh, H. Alghetaa, O. A. Abdulla, S. Chatterjee, P. B. Busbee, M. Nagarkatti, and P. Nagarkatti. 2019. AhR activation leads to massive mobilization of myeloid-derived suppressor cells with immunosuppressive activity through regulation of CXCR2 and microRNA miR-150-5p and miR-543-3p that target anti-inflammatory genes. J. Immunol. 203: 1830–1844.

- Mohammadi, S., A. Memarian, S. Sedighi, N. Behnampour, and Y. Yazdani. 2018. Immunoregulatory effects of indole-3-carbinol on monocyte-derived macrophages in systemic lupus erythematosus: a crucial role for aryl hydrocarbon receptor. *Autoimmunity* 51: 199–209.
- Li, S., X. Pei, W. Zhang, H. Q. Xie, and B. Zhao. 2014. Functional analysis of the dioxin response elements (DREs) of the murine CYPIAI gene promoter: beyond the core DRE sequence. Int. J. Mol. Sci. 15: 6475-6487.
- Chuang, H. C., C. Y. Tsai, C. H. Hsueh, and T. H. Tan. 2018. GLK-IKKβ signaling induces dimerization and translocation of the AhR-RORγt complex in IL-17A induction and autoimmune disease. Sci. Adv. 4: eaat5401
- 14. Ohtake, F., Y. Fujii-Kuriyama, K. Kawajiri, and S. Kato. 2011. Crosstalk of dioxin and estrogen receptor signals through the ubiquitin system. *J. Steroid Biochem. Mol. Biol.* 127: 102–107.
- Ohtake, F., Y. Fujii-Kuriyama, and S. Kato. 2009. AhR acts as an E3 ubiquitin ligase to modulate steroid receptor functions. *Biochem. Pharmacol.* 77: 474–484.
- Ohtake, F., A. Baba, Y. Fujii-Kuriyama, and S. Kato. 2008. Intrinsic AhR function underlies cross-talk of dioxins with sex hormone signalings. *Biochem. Biophys. Res. Commun.* 370: 541–546.
- Ohtake, F., A. Baba, I. Takada, M. Okada, K. Iwasaki, H. Miki, S. Takahashi, A. Kouzmenko, K. Nohara, T. Chiba, et al. 2007. Dioxin receptor is a ligand-dependent E3 ubiquitin ligase. *Nature* 446: 562–566.
- Stepankova, M., I. Bartonkova, E. Jiskrova, R. Vrzal, S. Mani, S. Kortagere, and Z. Dvorak. 2018. Methylindoles and methoxyindoles are agonists and antagonists of human aryl hydrocarbon receptor. Mol. Pharmacol. 93: 631-644.
- Brinchmann, B. C., E. Le Ferrec, W. H. Bisson, N. Podechard, H. S. Huitfeldt, I. Gallais, O. Sergent, J. A. Holme, D. Lagadic-Gossmann, and J. Øvrevik. 2018. Evidence of selective activation of aryl hydrocarbon receptor nongenomic calcium signaling by pyrene. *Biochem. Phar*macol. 158: 1–12.
- Zhao, B., D. E. Degroot, A. Hayashi, G. He, and M. S. Denison. 2010.
 CH223191 is a ligand-selective antagonist of the Ah (dioxin) receptor. *Toxicol. Sci.* 117: 393–403.
- Denison, M. S., A. A. Soshilov, G. He, D. E. DeGroot, and B. Zhao.
 Exactly the same but different: promiscuity and diversity in the molecular mechanisms of action of the aryl hydrocarbon (dioxin) receptor. *Toxicol. Sci.* 124: 1–22.
- Denison, M. S., and S. R. Nagy. 2003. Activation of the aryl hydrocarbon receptor by structurally diverse exogenous and endogenous chemicals. *Annu. Rev. Pharmacol. Toxicol.* 43: 309–334.
- Ehrlich, A. K., J. M. Pennington, W. H. Bisson, S. K. Kolluri, and N. I. Kerkvliet. 2018. TCDD, FICZ, and other high affinity AhR ligands dose-dependently determine the fate of CD4⁺ T cell differentiation. *Toxicol. Sci.* 161: 310–320.
- Pang, C., C. Zhu, Y. Zhang, Y. Ge, S. Li, S. Huo, T. Xu, R. H. Stauber, and B. Zhao. 2019. 2,3,7,8-Tetrachloodibenzo-p-dioxin affects the differentiation of CD4 helper T cell. *Toxicol. Lett.* 311: 49–57.
- Cho, S. W., K. Suzuki, Y. Miura, T. Miyazaki, M. Nose, H. Iwata, and E. Y. Kim. 2015. Novel role of hnRNP-A2/B1 in modulating aryl hydrocarbon receptor ligand sensitivity. *Arch. Toxicol.* 89: 2027–2038.
- Flaveny, C. A., and G. H. Perdew. 2009. Transgenic humanized AHR mouse reveals differences between human and mouse AHR ligand selectivity. Mol. Cell. Pharmacol. 1: 119–123.
- Mustafa, A., S. D. Holladay, S. Witonsky, D. P. Sponenberg, E. Karpuzoglu, and R. M. Gogal, Jr. 2011. A single mid-gestation exposure to TCDD yields a postnatal autoimmune signature, differing by sex, in early geriatric C57BL/6 mice. *Toxicology* 290: 156–168.
- Mustafa, A., S. D. Holladay, M. Goff, S. G. Witonsky, R. Kerr, C. M. Reilly, D. P. Sponenberg, and R. M. Gogal, Jr. 2008. An enhanced postnatal autoimmune profile in 24 week-old C57BL/6 mice developmentally exposed to TCDD. *Toxicol. Appl. Pharmacol.* 232: 51–59.



- Mustafa, A., S. D. Holladay, S. Witonsky, K. Zimmerman, C. M. Reilly,
 D. P. Sponenberg, D. A. Weinstein, E. Karpuzoglu, and R. M. Gogal, Jr.
 2009. Gestational exposure to 2,3,7,8-tetrachlorodibenzo-p-dioxin disrupts B-cell lymphopoiesis and exacerbates autoimmune disease in 24-week-old SNF1 mice. *Toxicol. Sci.* 112: 133–143.
- Needham, L. L., P. M. Gerthoux, D. G. Patterson, Jr, P. Brambilla,
 W. E. Turner, C. Beretta, J. L. Pirkle, L. Colombo, E. J. Sampson,
 P. L. Tramacere, et al. 1997. Serum dioxin levels in Seveso, Italy,
 population in 1976. Teratog. Carcinog. Mutagen. 17: 225–240.
- Liao, X., J. Ren, C. H. Wei, A. C. Ross, T. E. Cecere, B. S. Jortner, S. A. Ahmed, and X. M. Luo. 2015. Paradoxical Effects of all-transretinoic acid on lupus-like disease in the MRL/lpr mouse model. *PLoS One*. 10: e0118176.
- Lindén, J., S. Lensu, J. Tuomisto, and R. Pohjanvirta. 2010. Dioxins, the aryl hydrocarbon receptor and the central regulation of energy balance. Front. Neuroendocrinol. 31: 452–478.
- Mayer, C. T., S. Floess, A. M. Baru, K. Lahl, J. Huehn, and T. Sparwasser.
 2011. CD8⁺ Foxp3⁺ T cells share developmental and phenotypic features with classical CD4⁺ Foxp3⁺ regulatory T cells but lack potent suppressive activity. *Eur. J. Immunol.* 41: 716–725.
- 34. Kiniwa, Y., Y. Miyahara, H. Y. Wang, W. Peng, G. Peng, T. M. Wheeler, T. C. Thompson, L. J. Old, and R. F. Wang. 2007. CD8⁺ Foxp3⁺ regulatory T cells mediate immunosuppression in prostate cancer. *Clin. Cancer Res.* 13: 6947–6958.
- Houser, C. L., and B. P. Lawrence. 2022. The aryl hydrocarbon receptor modulates T follicular helper cell responses to influenza virus infection in mice. J. Immunol. 208: 2319–2330.
- Shinde, R., K. Hezaveh, M. J. Halaby, A. Kloetgen, A. Chakravarthy,
 T. da Silva Medina, R. Deol, K. P. Manion, Y. Baglaenko, M. Eldh,

- et al. 2018. Apoptotic cell-induced AhR activity is required for immunological tolerance and suppression of systemic lupus erythematosus in mice and humans. *Nat. Immunol.* 19: 571–582.
- Dorgham, K., Z. Amoura, C. Parizot, L. Arnaud, C. Frances, C. Pionneau, H. Devilliers, S. Pinto, R. Zoorob, M. Miyara, et al. 2015. Ultraviolet light converts propranolol, a nonselective β-blocker and potential lupus-inducing drug, into a proinflammatory AhR ligand. *Eur. J. Immunol.* 45: 3174–3187.
- Zhao, C. N., Z. Xu, G. C. Wu, Y. M. Mao, L. N. Liu, W. Qian, Y. L. Dan, S. S. Tao, Q. Zhang, N. B. Sam, et al. 2019. Emerging role of air pollution in autoimmune diseases. *Autoimmun. Rev.* 18: 607–614.
- 39. Dang, E. V.,, J. Barbi, H. Y. Yang, D. Jinasena, H. Y. Y. Zheng, Z. Bordman, J. Fu, Y. Kim, H. R. Yen, W. Luo, et al. 2011. Control of $T_H 17/T_{reg}$ balance by hypoxia-inducible factor 1. *Cell* 146: 772–784.
- Xiong, L., J. W. Dean, Z. Fu, K. N. Oliff, J. W. Bostick, J. Ye, Z. E. Chen, M. Muhlbauer, and L. Zhou. 2020. Ahr-Foxp3-RORγt axis controls gut homing of CD4⁺ T cells by regulating GPR15. Sci. Immunol. 5: eaaz7277.
- 41. Lee, J. H., C. Elly, Y. Park, and Y. C. Liu. 2015. E3 ubiquitin ligase VHL regulates hypoxia-inducible factor-1α to maintain regulatory T cell stability and suppressive capacity. *Immunity* 42: 1062–1074.
- 42. Rekik, R., M. Smiti Khanfir, T. Larbi, I. Zamali, A. Beldi-Ferchiou, O. Kammoun, S. Marzouki, S. Hamzaoui, S. Mrad, M. R. Barbouche, et al. 2018. Impaired TGF-β signaling in patients with active systemic lupus erythematosus is associated with an overexpression of IL-22. Cytokine 108: 182–189.
- 43. Sanjabi, S., L. A. Zenewicz, M. Kamanaka, and R. A. Flavell. 2009. Anti-inflammatory and pro-inflammatory roles of TGF-β, IL-10, and IL-22 in immunity and autoimmunity. *Curr. Opin. Pharmacol.* 9: 447–453.